

accepted for publication in PASP, Jan 2004

## Minimizing Strong Telluric Absorption in Near Infra-red Stellar Spectra

Matthew A. Kenworthy<sup>1</sup> and Margaret M. Hanson

*Department of Physics, University of Cincinnati, Cincinnati OH 45220*

[matt@physics.uc.edu](mailto:matt@physics.uc.edu)

### ABSTRACT

We have obtained high resolution spectra ( $R \sim 25000$ ) of an A star over varying airmass to determine the effectiveness of telluric removal in the limit of high signal to noise. The near infra-red line He I at  $2.058\mu\text{m}$ , which is a sensitive indicator of physical conditions in massive stars, supergiants, H II regions and YSOs, resides among pressure broadened telluric absorption from  $\text{CO}_2$  and water vapor that varies both in time and with observed airmass.

Our study shows that in the limit of bright stars at high resolution, accuracies of 5% are typical for high airmass observations (greater than 1.9), improving to a photon-limited accuracy of 2% at smaller airmasses (less than 1.15). We find that by using the continuum between telluric absorption lines of a ro-vibrational fan a photon-limited 1% accuracy is achievable.

*Subject headings:* techniques: spectroscopic — methods: data analysis

### 1. Introduction

Our goal is to obtain high quality moderate resolution spectra ( $R \sim 10000 - 20000$ ) to be used in conjunction with sophisticated stellar model atmospheres (Santolaya-Rey, Puls & Herrero 1997). The near infra-red (NIR) spectrum of the atmosphere from  $1 - 5 \mu\text{m}$ , is dominated with telluric water and  $\text{CO}_2$  absorption, between which the major observing windows in the wavelength region are defined. Broad molecular absorption bands of  $\text{CO}_2$  are resolved at moderate spectral resolution ( $R > 5000$ ) into individual pressure broadened ro-vibrational transitions. These transitions vary both in time and observed elevation making their removal problematic in ground based spectroscopic studies.

---

<sup>1</sup>Steward Observatory, 933 North Cherry Avenue, Tucson, AZ 85721

There is a tremendous motivation from astronomers to obtain highly accurate spectral profiles for lines existing in the near-infrared. For hot stars, an important line in modeling extended atmospheres and stellar winds is the He I transition at  $2.058\mu\text{m}$  (Hanson et al. 1996). This line is also an important diagnostic in H II regions (Lumsden et al. 2003), massive young stellar objects (Porter et al. 1998) and planetary nebulae (Depoy & Shields 1994; Lumsden et al. 2001). However, the line is located near the short wavelength edge of the K band window, where  $\text{CO}_2$  absorption bands dominate the spectrum. The challenge for observational astronomers is in observing the  $2.058\mu\text{m}$  line profile with high signal to noise suitable for detailed modeling despite considerable telluric contamination.

Observations of standard stars are essential to obtain even modest correction of telluric absorption features in this spectral region. This paper investigates the variability of the telluric absorption near the He I transition and discusses the limits to the signal to noise ratio achievable given a typical observing program and instrument. We follow an A2V star for half a night through a range of airmasses and see what effect the variation of telluric absorption has on the recovered spectra.

## 2. Observations

The data were taken at the IRTF on 2003 June 08 0600 UT (2003 June 07 2000 HST). Meteorological data from weather stations across the Mauna Kea summit are shown in Figure 1 along with the range of airmasses observed. The observations started at an airmass of 1.95 and finished at an airmass of 1.13, when the star was approaching transit.

We use the CSHELL echelle spectrograph (Greene et al. 1993) with a slit width of 1.0 arcsec. Combined with the pixel scale of 0.2 arcsec/pixel, this gives a slit width of 5 pixels on the  $256 \times 256$  ( $30\mu\text{m}$  pitch) InSb array. The array has a read noise of  $55e^-$  per pixel per sample, and a dark current of  $0.5 e^-$  per second per pixel with an approximate gain of  $11 e^-/\text{ADU}$ . With a 325mV bias, it is 1% linear at  $22,000e^-$ . One echelle order is selected with an order sorting filter, and the dispersion is  $0.20\text{\AA}/\text{pixel}$ . Due to problems with the telescope guiding camera, the telescope is off-axis guided by a nearby star, in contrast to the usual mode of on-axis guiding with the target star in the visible.

The dispersion of the spectrograph at  $2.0563\mu\text{m}$  is measured at  $0.207\text{\AA}/\text{pixel}$ . The instrumental spectral resolving power is measured by fitting a Gaussian to two OH night sky emission lines, identified as a  $\Lambda$  P1 doublet (Rousselot et al. 2000), with a full width half maximum (FWHM) of 4.0 pixels (12.1km/s) with the star overfilling the slit. This gives a higher spectral resolution than expected with the stated slit width, and so we take our measured value of the dispersion and instrumental width to obtain a spectral resolution of 24,800.

A dwarf A2 star is not expected to have any significant metal lines in its spectrum, and as a result acts as a continuum source above the atmosphere over the spectral region of the study. The

A2V star HD 156729 ( $17^{\text{h}}17^{\text{m}}40.2545^{\text{s}}$ ,  $+37^{\circ}17'29.39''$ , J2000,  $V = 4.62$ ) is followed from an airmass of 1.95 through to 1.13 with 30 second integrations in a continuous beam switching mode with a throw of  $9.0''$ . The mean time between the start of successive observations is 34 seconds, resulting in 268 fully reduced observations.

We set the central wavelength of the spectra to  $2.061\mu\text{m}$  to include a range of different line strengths. Three P branch transitions, the Q transition, and four R branch transitions of CO<sub>2</sub> are included in the spectra, along with some H<sub>2</sub>O transitions (see Fig. 2).

A set of twenty flat fields is taken immediately after the end of the observations, using a continuum lamp placed in front of the entrance slit of the spectrograph. Dark frames of identical duration to the flat field exposures are taken later in the night.

### 3. Reduction of the Echelle Spectra

All spectra are reduced using **IRAF**<sup>2</sup> routines, and subsequent analysis is done using **PerlDL**<sup>3</sup>.

The dark frames and flat field frames are averaged together to form a master dark frame and master flat frame and frames showing the r.m.s. per combined pixel (sigma frames) are produced. The master dark frame is subtracted from the master flat field frame, and the flat field is normalized in the spectral direction to produce a pixel response frame. Bright, noisy and dead pixels are identified using the sigma frames, and a bad pixel frame is generated for the detector. Pairs of science frames are subtracted from each other, divided by the pixel response frame and then bad pixels flagged in the bad pixel frame are interpolated over using data from the surrounding good pixels.

There are two spectra per beam-switched frame. A fixed aperture width of 24 pixels (corresponding to  $4.8''$ ) is used to extract the spectra from the frame. Although in ideal beam switching the frame background level is zero, we noted in four pairs of beam-switched frames that a jump in bias level in the readout of the frame would result in a zero level offset of up to 20 counts being present in the data, compared with the typical flux of 200 counts per pixel in the spectrum. Visual examination of these images show a very smooth background that is automatically subtracted as part of the spectral extraction. Remaining transient events are removed using the 'clean' algorithm in the spectral extraction package, using the known gain and effective read noise of the beam switched images. The centroid position of the spectra are traced with a third order Legendre function.

Wavelength dispersion correction is performed using the telluric profiles themselves. A model

---

<sup>2</sup>IRAF is distributed by the National Optical Astronomy Observatories, which are operated by the Association of Universities for Research in Astronomy, Inc., under cooperative agreement with the National Science Foundation.

<sup>3</sup>homepage at: <http://pdl.perl.org/>

of the atmospheric transmission is generated for the observing site using ATRAN (Lord 1992) and all absorption line profiles are measured from this reference. These are then used to wavelength calibrate the individual spectra. Using a second order Legendre function, a wavelength solution with rms fit of  $0.03\text{\AA}$  is typical, corresponding to a goodness of fit of about 1/10 of a pixel. The absorption lines are labeled according to the HITRAN database (Rothman et al. 2003) in Figure 2.

#### 4. Observing Technique

The telluric absorption in the NIR varies as a function of airmass and of time (Tokunaga 1999). Ideally, in spectral regions of strong telluric absorption, a standard star and a science target should be observed through identical atmospheric paths at the same time, allowing the atmospheric absorption to be divided out. In this perfect case, a reference star would be within a few arcseconds of a science target, and placing the spectrograph slit across both objects in a position suitable for beam-switching would result in the highest observing efficiency and accuracy.

Bright stars with no metallic lines (usually those later than B8V and earlier than A2V), are the most appropriate for telluric removal. They are not perfect in that these stars have broad Hydrogen lines in their spectra and to obtain science target spectra in these regions, various modeling techniques have been developed (Maiolino et al. 1996; Hanson et al. 1996; Vacca et al. 2003) to remove the Hydrogen lines from the standard star spectra whilst preserving the (much narrower) telluric absorption lines.

##### 4.1. Standard star observations at different airmasses

A complete observation consists of spectra of the science target, slewing the telescope to a nearby standard star, and taking spectra of the standard star. The standard star and science target observations are separated both in time and position on the sky, and so are observed through different paths in the atmosphere. Differences in the telluric absorption between these two pointings result in systematic errors appearing in the science object spectra, and these can significantly reduce the signal to noise and sensitivity reached in the object spectrum. This is shown in Figure 3, where the ratios of standard star spectra at 1.13 and 1.94 airmasses is shown. The two lower spectra show the ratio of spectra taken approximately 35 seconds apart, with the lowest spectrum at 1.13 airmasses and the middle spectrum at 1.94 airmasses. The spectra show a flat, Gaussian noise dominated continuum, with spike-like residuals located at the cores of telluric absorption lines. This effect is seen in greater detail in the topmost spectrum, where the ratio is between a spectrum from 1.13 and 1.94 airmass.

The root mean squared value of such normalized spectra is a measure of the standard deviation of the spectrum from its mean value. Various sources of noise combine together in quadrature to

give the theoretical lowest noise limit attainable for a given spectral element in the final spectrum. For our ratioed spectra, we calculate a theoretical signal to noise ratio and compare it to the measured signal to noise ratio. The noise sources we include in the calculation of the theoretical noise limit are detector read noise, photon count noise, and flat field noise. For our extraction width of 24 pixels this corresponds to a read noise of  $380e^-$  per wavelength bin of a beam-switched image, and our flat field signal to noise ratio is approximately 1200.

The increase in airmass difference between the two spectra leads to lower signal to noise, as seen in Figure 4. At low airmass, the theoretical limit of 2.3% is reached for exposures taken one minute apart (the filled circles). However, at a higher airmass of 1.94 (hollow circles), its theoretical limit of 2.6% is NOT reached, and instead the noise tails off at 5%, a signal to noise ratio of only 20. Seeing the significant telluric residuals for 1.94 airmasses in the middle spectrum of Figure 3, it is apparent that as low as possible an airmass should be used for both standard and science object.

We also examine the standard deviation of the spectrum as a function of airmass difference for a region of the spectrum with small telluric absorption,  $2.0602 - 2.0608\mu\text{m}$ . The theoretical noise limit of 1% is reached (Figure 5) and for large airmass differences there is only a small decrease in signal to noise. Clearly, high signal to noise infra-red spectra are obtainable in regions free of telluric absorption.

#### 4.2. Removing the residual telluric line features in oversampled spectra

Figure 6 shows the He I absorption in a O7Ib supergiant with data taken on 07 June 2003 UT. The science target is HD 192639 observed at 1116UT at an airmass of 1.21 and the reference star is HD 195050 observed at 1050UT at an airmass of 1.36. The spectra are wavelength calibrated using the telluric absorption lines. The broad stellar absorption is clearly visible after dividing out the telluric lines. The residual spikes are due to the change in airmass and the telluric profile structure between the two exposures.

We investigated different methods for removing the residuals, which include simple Fourier filtering, clipping, and modeling.

We oversample our spectra above the Nyquist frequency of 2.5 pixels per spectrally resolved element, and our measured sampling (the instrumental profile) is 4.0 pixels. This, then, is the narrowest feature that the spectrograph can resolve for any spectral line source. The telluric residuals in Figure 6 arise from small changes in the shape of the line profile of the telluric absorption, and subsequent division of the science object by the standard source gives rise to large flux changes over very small wavelength intervals. These are usually smaller than the instrumental profile, and can be readily identified in the final spectra. By comparing to a known list of telluric absorption lines and to the standard star spectrum, regions of poor signal to noise corresponding to the core of the telluric lines can be identified and interpolated over using a low pass filter.

Another hypothesis is that the large residual spikes are due to a systematic wavelength shift errors between the two spectra. To study the effect of introducing a systematic wavelength shift in one of the two spectra, we take a detailed portion of the spectrum in Figure 6 and add a wavelength offset to the science star spectrum before dividing by the standard star. The results of adding a range of shifts is shown in Figure 7. Clear P Cygni-type profiles appear for even small wavelength offsets, indicating that accurate wavelength calibration is necessary for high spectral resolution work of this type. On the right hand side of the spectrum, telluric residuals of up to 40% of the continuum remain for all displayed shifts, whilst other telluric lines cancel out to give a flat continuum at other wavelengths. We confirmed this by dividing the A star spectra at airmasses similar to those of HD 192639 and its standard star, confirming the need to match airmasses of scientific targets.

The almost constant wavelength spacing of the telluric lines in the ro-vibrational bands suggests some form of Fourier filtering to remove the residuals. We find that there is no effective way to remove all the residual lines without degrading the line profile on astrophysical lines of interest, and so we do not recommend Fourier filtering as an effective way of removing the residuals. It is best to manually interpolate over known telluric absorption features and then use a piecewise spline to supply replacement values over regions of low signal to noise.

## 5. Conclusions

The near-infrared spectral region provides a number of diagnostic transitions important for the analysis of a variety of astronomical objects. Yet, ground based observations are plagued with the removal of numerous, varying and sometimes very strong absorption features originating in the Earth’s atmosphere. We investigate the telluric absorption as a function of airmass. Naturally, in the limit of bright stars and high spectral resolution, the greater the airmass difference between the science target and the reference star, the lower the resultant signal to noise achieved in the final spectrum and the greater the contamination of systematic residuals from the telluric line wings. However, we also show that observations at higher airmasses are degraded due to the larger rate of change of airmass with time, and with the greater path length through the atmosphere. We find that a signal to noise ratio of 20 (5%) is achievable for targets at airmasses of around 1.9, increasing to a SNR of 50 (2%) for observations near an airmass of 1.15.

We conclude that high signal-to-noise (100 and greater) spectra of astrophysical spectral lines whose wavelengths and line widths coincide with the cores and widths of some of the deepest telluric absorption is impossible to achieve with the observing technique described in this paper. The variability of the telluric lines combined with the large flux attenuation and necessarily long integration times mean that only simultaneous observations with standards can compensate for the effects of the atmosphere.

By using high spectral resolution spectra, regions of low absorption between the telluric lines

are able to reach near photon-limited sensitivities (down to 1%), and for spectral features that are significantly broader than telluric features, high signal to noise spectra are possible.

Thanks go to John Rayner and Paul Sears at the IRTF, and to Tom Greene and Tom Geballe for their suggestions and additional insight. We also thank our anonymous referees for their comments and corrections. This work is supported by the National Science Foundation under grant AST 00-94050 to the University of Cincinnati.

## REFERENCES

Depoy, D.L., Shields, J.C. 1994, *ApJ*, 422, 187

Greene, T.P., Tokunaga, A.T., Toomey, D.W., Carr, J.S. 1993, *SPIE*, 1946, 313

Hanson, M.M., Conti, P.S., Rieke, M.J. 1996, *ApJS*, 107, 281

Lord, S.D. 1992 A New Software Tool for Computing Earth's Atmospheric Transmission of Near- and Far-Infrared Radiation, NASA Technical Memorandum 103957

Lumsden, S.L., Puxley, P.J., Hoare, M.G., Moore, T.J.T., Ridge, N.A. 2003, *MNRAS*, 340, 799

Lumsden, S.L., Puxley, P.J., Hoare, M.G. 2001, *MNRAS*, 320, 83

Maiolino, R., Rieke, G.H., Rieke, M.J. 1996, *AJ*, 111, 537

Porter, J.M., Drew, J.E., Lumsden, S.L. 1998, *A&A*, 332, 999

Rothman, L.S. et al., 2003, *Journal of Quantitative Spectroscopy and Radiative Transfer*, 82, 5-44

Rousselot, P., Lidman, C., Cuby, J.-G., Moreels, G. and Monnet, G. 2000, *A&A*, 354, 1134

Santolaya-Rey, A. E., Puls, J., Herrero, A. 1997, *A&A*, 323, 488

Tokunaga, A.T. 1999, *Allen's Astrophysical Quantities*, 4th ed., A.N. Cox, New York: AIP Press, 143

Vacca, W.D., Cushing, M.C., Rayner, J.T. 2003, *PASP*, 115, 389

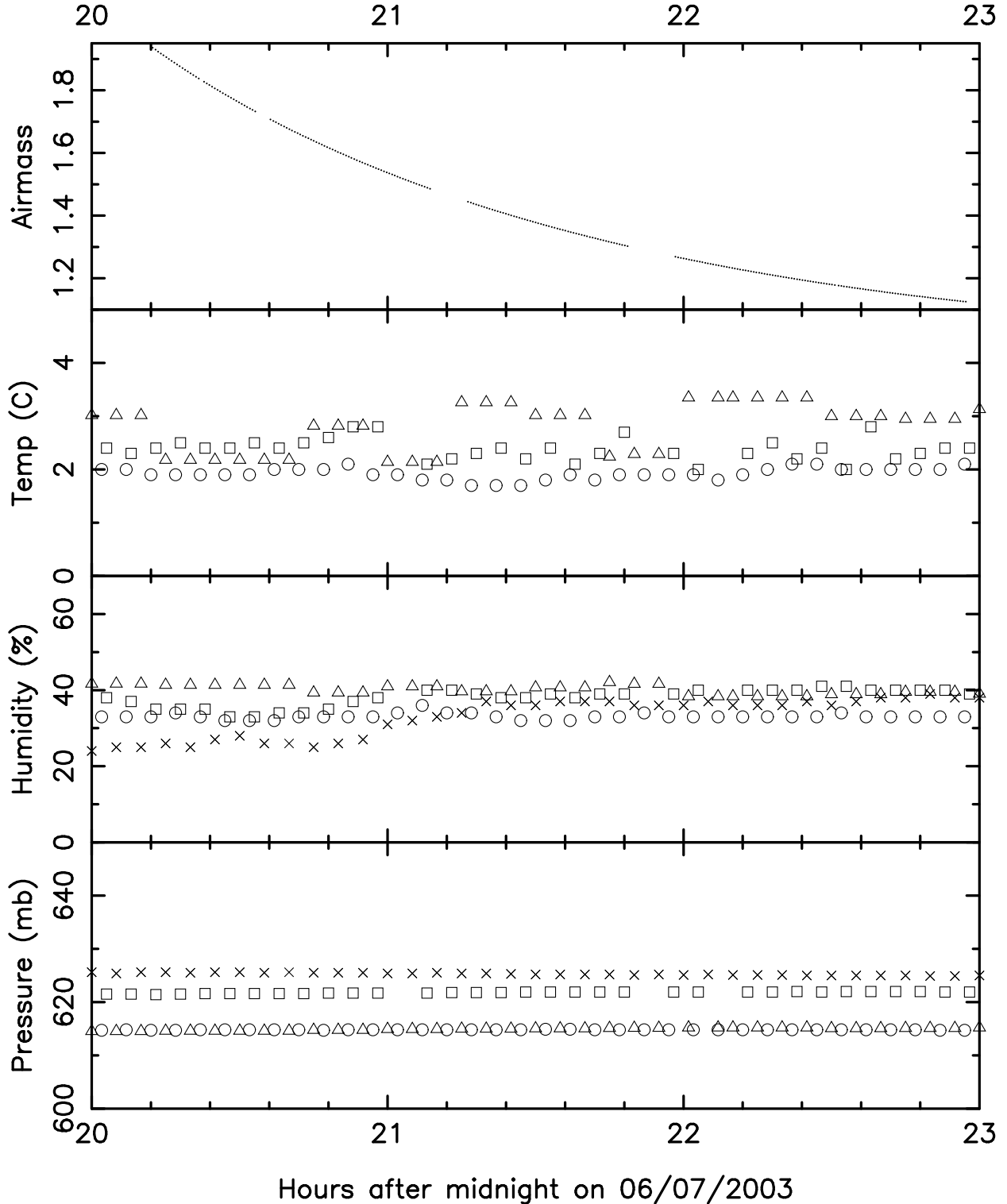


Fig. 1.— Meteorological conditions from different telescope weather stations across the summit of Mauna Kea. CFHT data are marked with a circle, CSO with a cross, Subaru with a square, and UKIRT with a triangle. Data provided by Mauna Kea Weather Center (Lyman 2003, priv. communication).

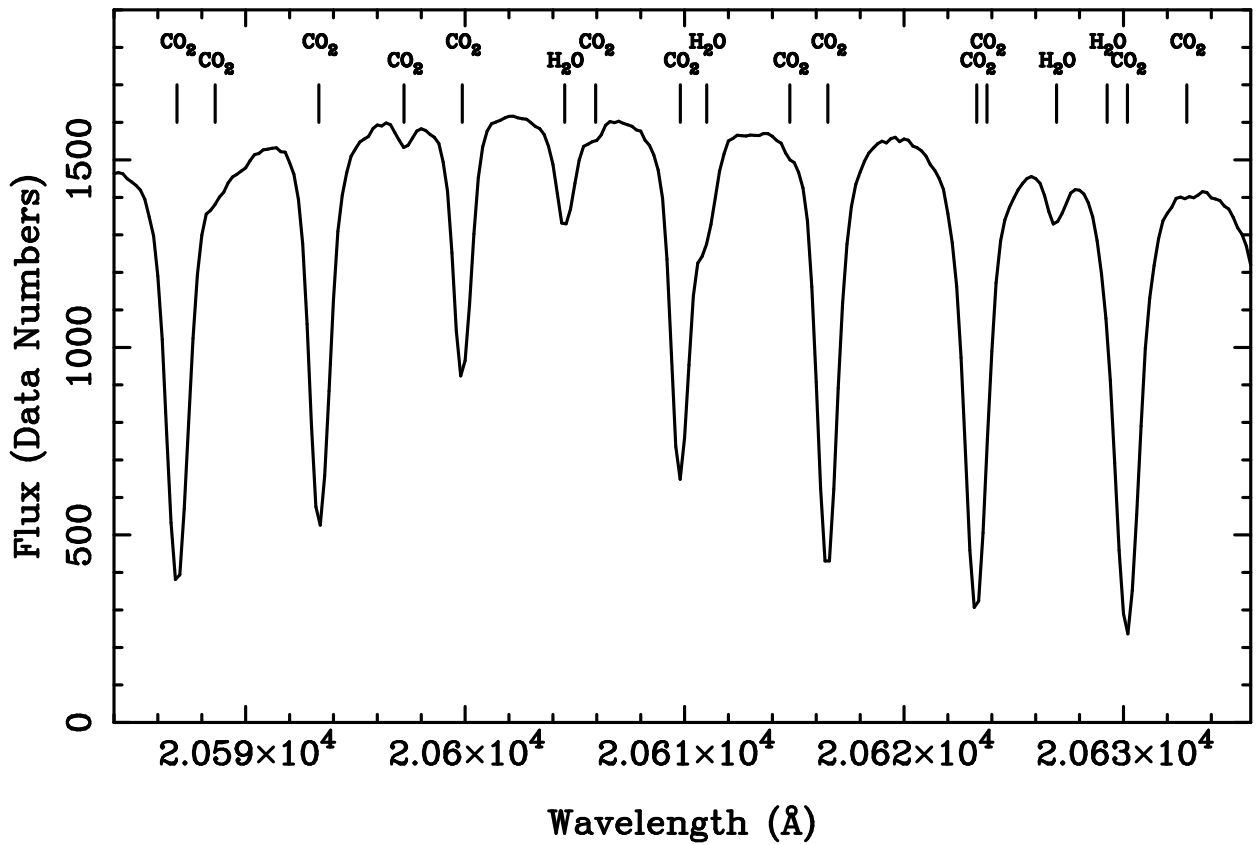


Fig. 2.— Spectrum of an A2V star, averaged from 10 exposures at a mean airmass of 1.13. All spectral features are due to telluric absorption in the Earth's atmosphere. Lines are identified according to the HITRAN database (Rothman et al. 2003). Echelle transmission function has not been removed from the spectrum.

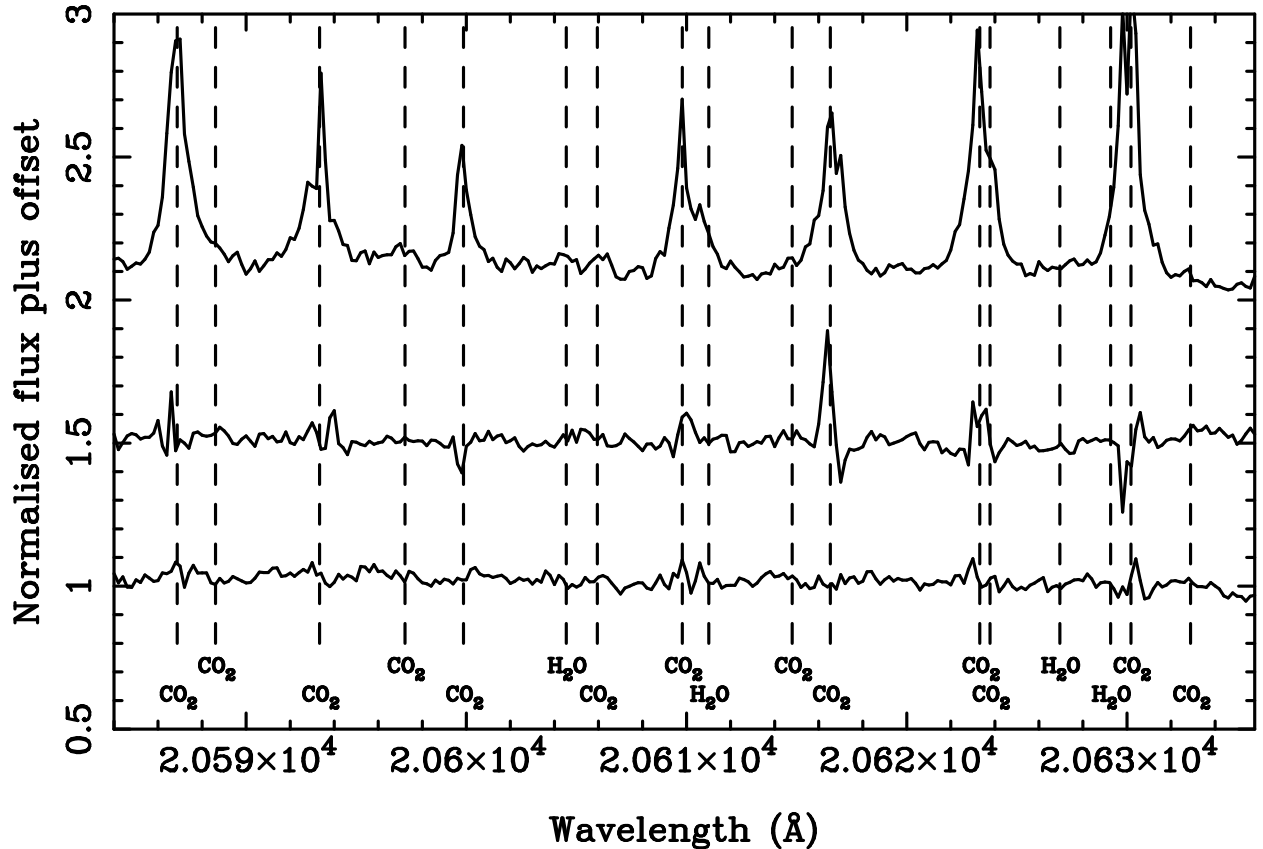


Fig. 3.— The ratio of two spectra of the same star taken at different airmasses. The lowest spectrum is the division of two spectra taken at an airmass of 1.13. The middle spectrum is the division of spectra taken at an airmass of 1.94, and the top spectrum shows the division of a spectrum at an airmass of 1.13 by a spectrum at 1.94. Each spectrum has been offset by a flux of 0.5, and the dashed lines mark the center of telluric absorption lines and their associated molecular species.

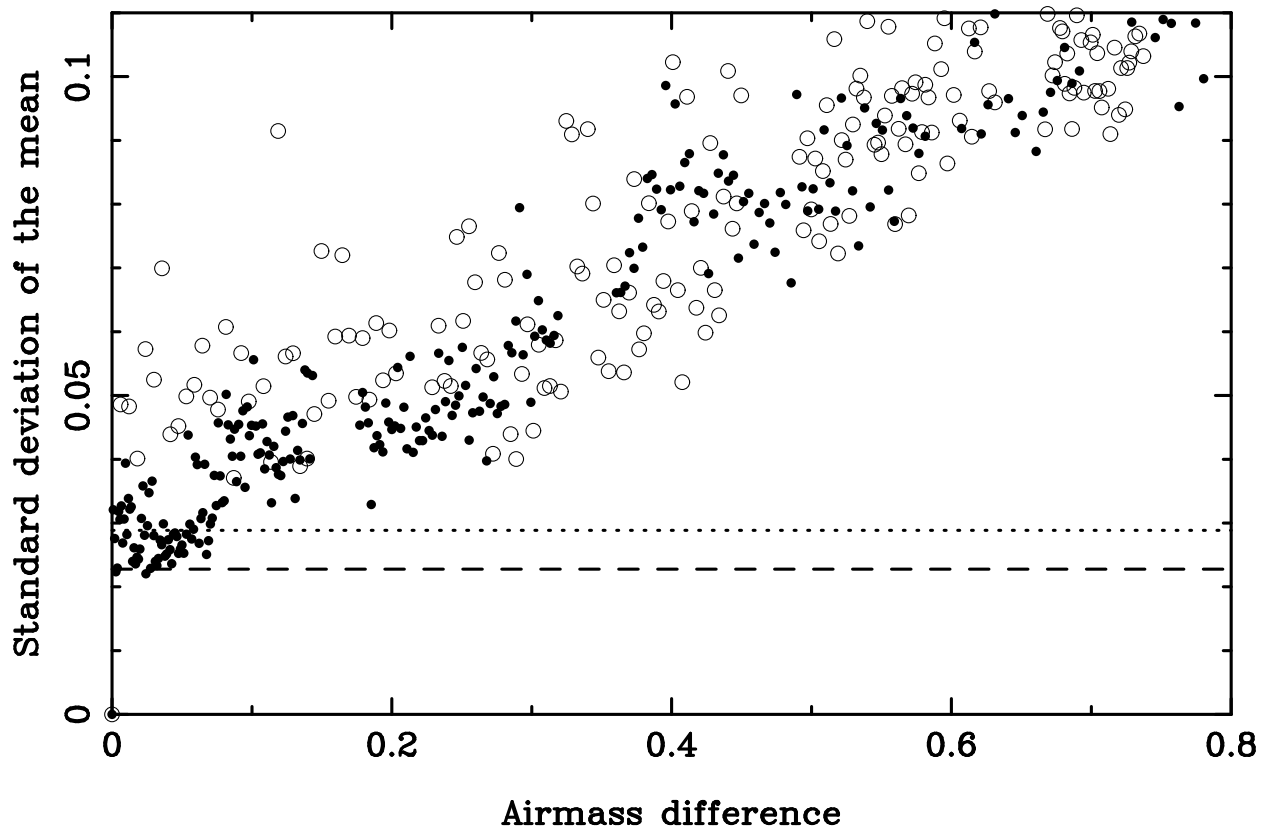


Fig. 4.— A graph showing the standard deviation of the mean of the ratio of a standard star taken at two different airmasses, over a wavelength range of  $2.0584 - 2.0636\mu\text{m}$ . Filled circles relative to an airmass of 1.13, hollow circles relative to an airmass of 1.94. The dashed line represents the theoretical signal to noise attainable for observations at an airmass of 1.13, the dotted line is the same but for an airmass of 1.94.

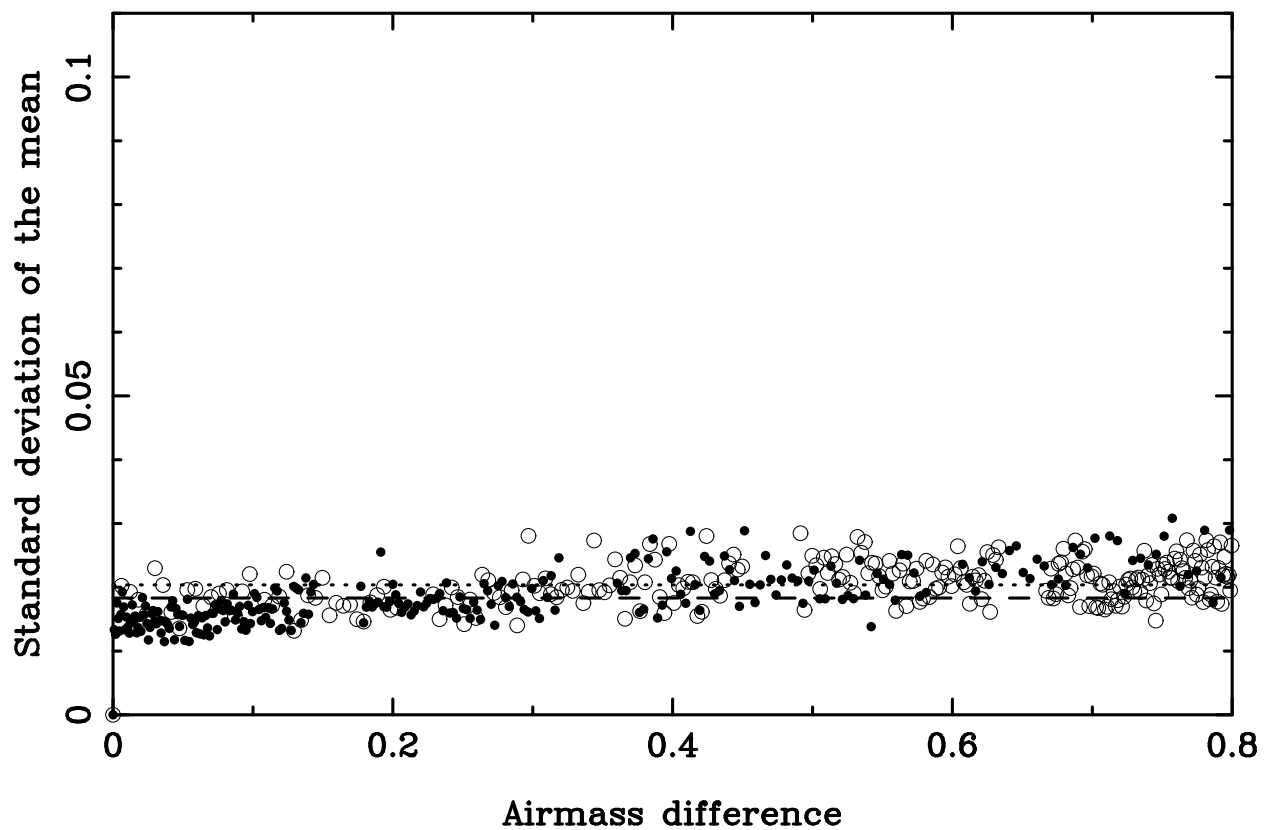


Fig. 5.— Same as Figure 3 but over the range of  $2.0602 - 2.0608\mu\text{m}$ .

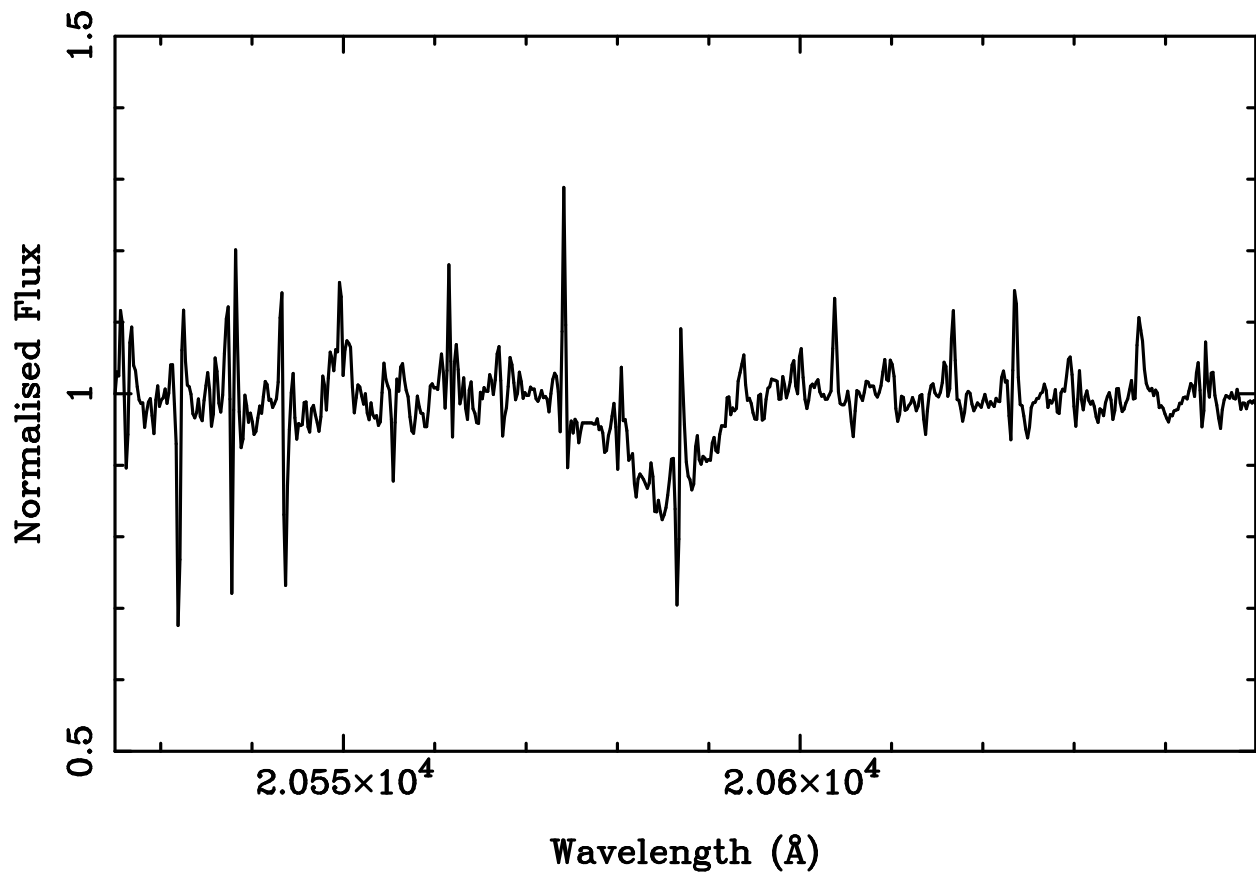


Fig. 6.— Spectrum of HD 192639. Residuals from the division of the standard are visible, along with the broad absorption from He I at  $2.058\mu\text{m}$ .

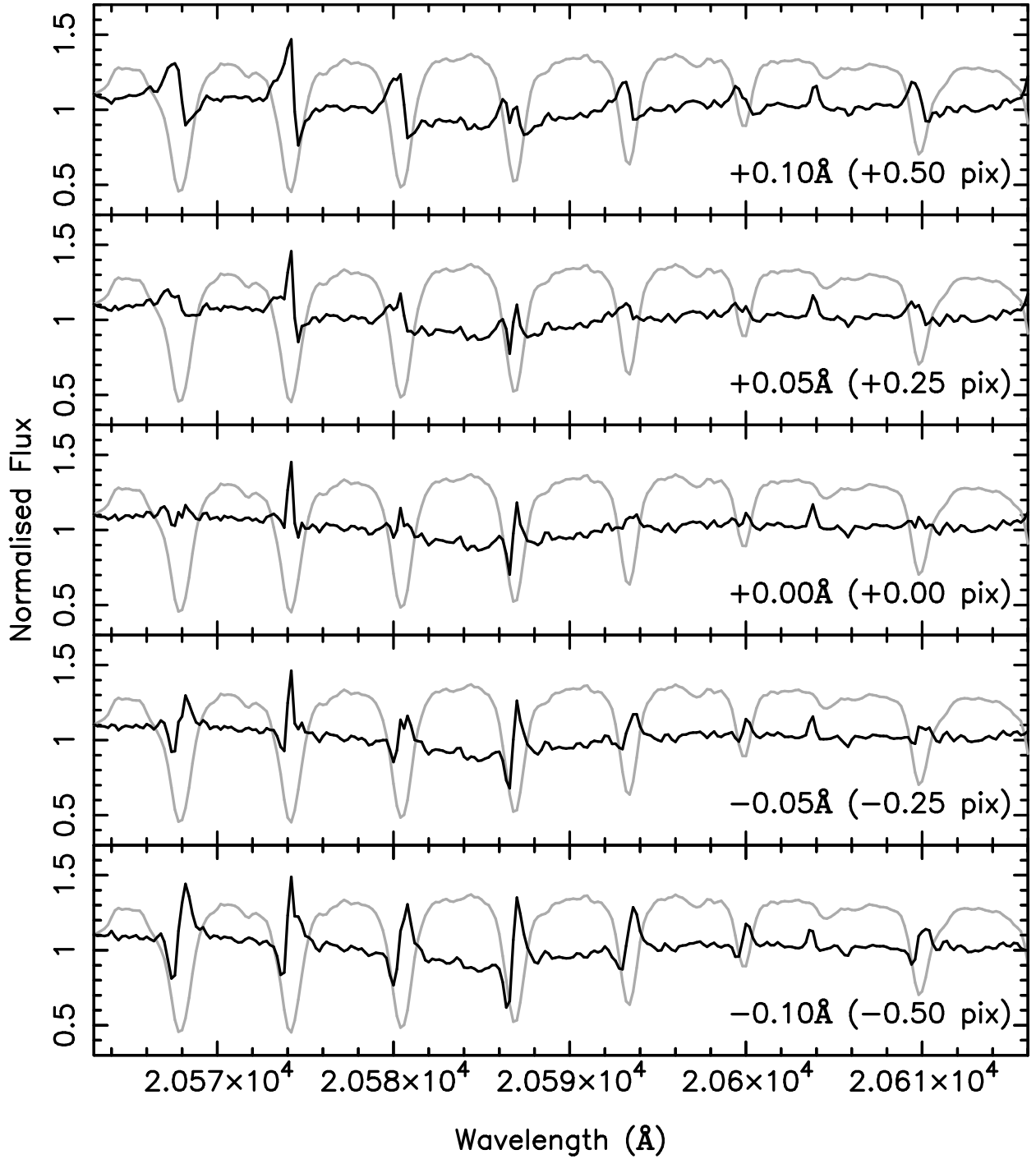


Fig. 7.— Spectrum of HD 192639 as a function of different wavelength misalignments. In each panel, the spectrum of HD 192639 is offset by the amount indicated in the lower right corner before division by the standard star spectrum. The standard star spectrum is shown in light gray to the same scale and with a flux offset of +0.3.